Asian Journal of Chemistry; Vol. 28, No. 7 (2016), 1501-1504

ASIAN JOURNAL OF CHEMISTRY

http://dx.doi.org/10.14233/ajchem.2016.19739

Probing the Nature of Defects of Graphene like Nano-Carbon from Amorphous Materials by Raman Spectroscopy

ANU N. MOHAN[1,2], B. MANOJ[1,*] and A.V. RAMYA[1]

[1]Department of Physics, Christ University, Bangalore-560 029, India
[2]Department of Physics, Jain University, Bangalore-560 001, India

*Corresponding author: E-mail: manoj.b@christuniversity.in

Received: 24 November 2015; *Accepted*: 10 February 2016; *Published online*: 31 March 2016; AJC-17837

Raman spectral characterization of selected carbonaceous materials has been carried out at excitation wavelengths 514, 633 and 1064 nm. Raman studies exhibit the presence of G band owing to the first order of E_{2g} mode scattering. sp^3 domains at about 1355 cm^{-1} (D band) are ascribed to the disordered structures due to the on-site and hoping defects which introduces distortions in the crystal lattice. Spectral de-convolution indicates the prominence of bands namely G, D1, D2, D3 and D4. D3 and D4 bands follow Gaussian, while the others Lorentian distribution. With change in excitation wavelength of laser, the degree of dispersion of G peak and I_D/I_G intensity ratio are found to increase. The crystallite size L_a, shows an inverse relation with intensity of defect to graphite band (I_D/I_G) and it also obeys Tuinstra-Koenig relation for nano-crystalline substance. The lateral size of aromatic lamellae determined using XRD analysis is in good agreement with that of Raman analysis. The feasibility of using kerosene soot, diesel soot and carbon black for electrochemical applications are also explored.

Keywords: Graphene layers, Graphitic band, Defect band, Carbon.

INTRODUCTION

Graphene is the fundamental block of all sp^2 carbon allotropes which can be stacked to graphite, rolled to nanotubes or wrapped to get fullerene structure [1-3]. In spite of having qualities like inertness and ultrahigh strength, graphene structures possess various incorporated defects. These defects breaks the symmetry of lattice structure which mainly includes vacancies, grain boundaries or changes associated with the graphitic to diamond hybridization. The extent of these defects depends on the synthesis route and the precursors. These defects have a major effect on the characteristics of graphene thereby tampering the electron mobility and chemical reactivity of graphene. Hence, probing the precise nature and consequences of such structural defects is of utmost importance in the current application oriented domains.

For the structural characterization of graphitic like carbon, diffraction techniques are ideal, while for disordered materials, Raman spectroscopy is theapttool [4-11]. Raman spectroscopy is sensitive to crystal structure and short-range ordering of nano-carbon. The shapes, intensities and positions of prominent Raman peaks provide vital information about the types of carbon structures present. Raman spectroscopy provides details about the defect bands in the spectrum along with G and 2D band. Graphene like nano carbon is a perfect candidate to probe disorder because its 2D-structure makes it easier to alter the carbon skeleton and introduce defect in it. In the present paper, an attempt has been made to elucidate the structure of defect-incorporated carbon network in selected amorphous carbon and carbon black with Raman spectroscopy. The obtained spectral parameters, its dependence on excitation wavelength and various other structural information are presented.

EXPERIMENTAL

Soot obtained from two different hydrocarbons (kerosene and diesel) along with carbon black (CB) are the selected amorphous materials to investigate the monolayer formation by Raman spectroscopy. Soot, prepared by thermal decomposition of the precursors in a controlled environment was dispersed in water and sonicated at 33 MHz for 30 min to remove agglomeration. The spectral features of samples were analyzed by a Raman spectrometer (Horiba Jobin Lab RAM HR system) in the back scattering mode with three different excitation wavelength (λ = 514 nm, a 632.8 nm and 1064 nm). Spectral de-convolution was performed using Origin pro8 software.

RESULTS AND DISCUSSION

First order Raman spectra of the soot samples recorded at a wavelength of 514 nm were de-convoluted to know the nature of constituent carbon (Figs. 1-3). When the disorder is moderate in a graphene system, the ratio of intensities of D and D′ peaks ($I_D/I_{D'}$) gives an insight about the nature of defect. This intensity ratio is closely related to the amount of defect present. I_D/I_G, $I_D/I_{D'}$ and $I_{D'}/I_G$ ratios for all the samples are tabulated in Table-1.

TABLE-1
DEPENDENCE OF DEFECT TO GRAPHITIC PEAK

Sample	I_D/I_G	$I_D/I_{D'}$	$I_{D'}/I_G$
Kerosene soot	0.95	3.00	0.32
Diesel soot	1.66	2.55	0.65
Carbon black	0.58	0.90	0.64

Eckmann *et al.* [6] simulated three types of defects in graphene system namely i) hoping defect- originating from the distortion of carbon bond ii) on-site-defect-arising due to the out-of-plane atoms bonded to carbon atoms describing the sp^3 hybridized phase and iii) charged impurity-resulting from the presence of charged impurities. The reported value of $I_D/I_{D'}$ is about 10.5 for the hopping defect while it is about 1.3 for the on-site defects. $I_D/I_{D'}$ ratio is found to be 3, 2.55 and 0.9 for the kerosene soot, diesel soot and carbon black samples, respectively (Table-1). This indicates that in carbon black, the defect is mainly due to on-site defect while in the other two samples the defect is attributed to the combination of on-site and hopping defects.

The prominent features in the Raman spectrum of kerosene soot (Fig. 1) are the graphitic band appearing at 1591 cm^{-1} (G), the defect band at about 1334 cm^{-1} (D) and the D′ band at about 1610 cm^{-1} (D2 band).

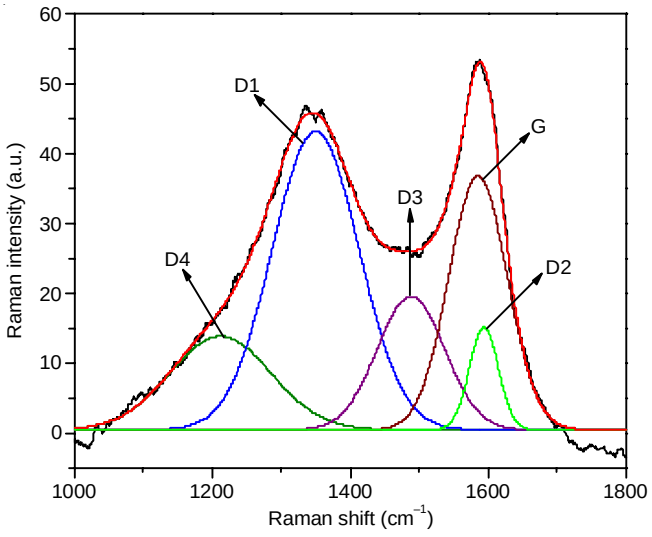

Fig. 1. Raman spectrum of kerosene soot

Raman analysis of diesel soot is presented in Fig. 2. The peak observed at 1583 cm^{-1}, unveils the presence of E_{2g} mode of graphite like structure. D band is very weak, confirming low level of defects in the crystal lattice. The relative intensity ratio of the defect and graphite bands was found to be 1.15,

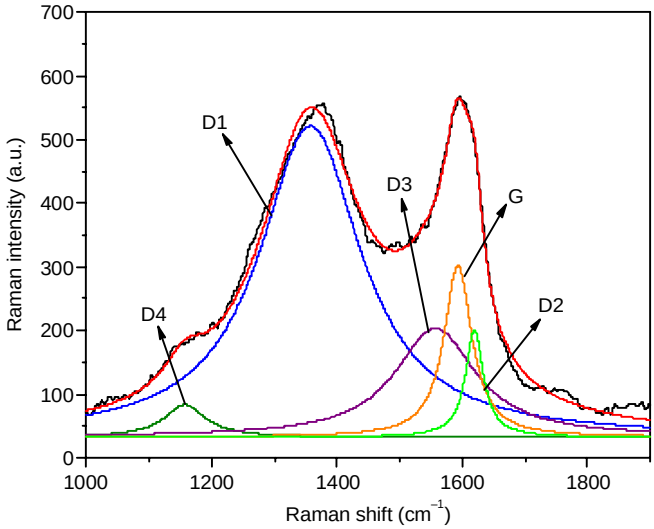

Fig. 2. Raman spectrum of diesel soot

while the lateral size of the aromatic lamellae was calculated as 4.57 nm.

Raman spectrum of carbon black (Fig. 3) portray a weak band at 1328 cm^{-1} corresponding to D band while the G band is appearing at 1597 cm^{-1}. The ratio of defect to graphitic band is found to be 0.58, establishing the high degree of graphitic carbon content in the sample.

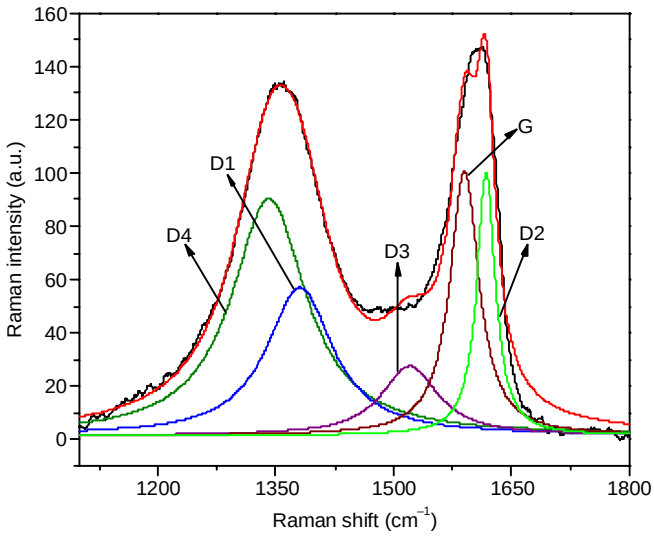

Fig. 3. Raman spectrum of carbon black

Raman analysis by spectral de-convolution: Upon deconvolution of the first order spectrum, five bands are observed (Figs. 1-3). The peak at 1585 cm^{-1} (G) has an additional D2 band, originating from graphitic like planes [1-4]. The band at about 1500 cm^{-1} (D3) initiates from the amorphous part of soot. Jawhari *et al.* [5] proposed a Gaussian line shape for this band owing to the statistical distribution of carbon in the distorted graphitic lattice. The peaks at about 1350 cm^{-1} (D1) and about 1200 cm^{-1} (D4) are attributed to the presence of sp^2-sp^3 mixed phase of the carbon.

Dependence of structural parameters on excitation wavelength: Raman spectra of kerosene soot, diesel soot and carbon black were recorded with two more wavelengths (1064

and 633 nm) to determine the dependence of structural parameters on the excitation wavelength (Figs. 4-7). In finite crystallites, D band will be red shifted with increase in excitation (from 1284 to 1327 cm^{-1} as the degree of ordering of carbon structure decreases). The D peaks observed for kerosene soot (1279 cm^{-1}), carbon black (1275 cm^{-1}) and diesel soot (1297 cm^{-1}) confirmed high degree of ordering of nanomaterial formed in the combustible product. For diesel soot, a band at 2882 cm^{-1} (designated as 2D band; shifts to longer wavenumbers as carbon structure becomes ordered) was observed, apart from the E_{2g} band (1596 cm^{-1}) at wavelength of 1064 nm [9]. 2D band, overtone of D band is normally present at 2607 cm^{-1} for crystalline carbon [10-15]. The 2D band is displaced to lower wavelength in diesel soot, while in carbon black, an opposite trend is observed.

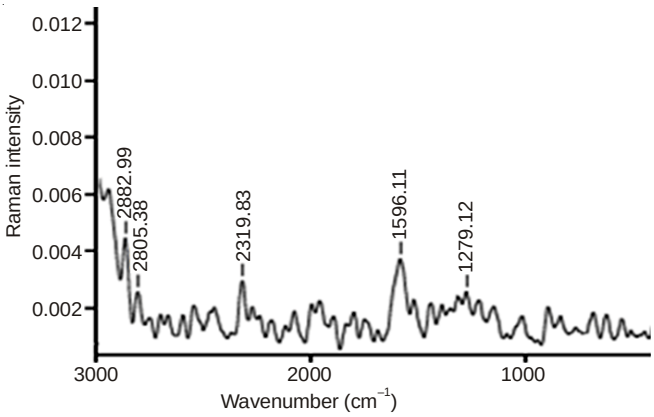

Fig. 4. FT-Raman spectrum of kerosene soot

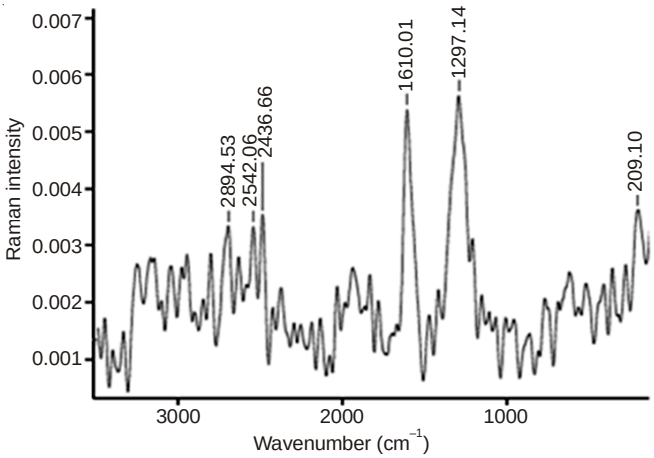

Fig. 5. FT-Raman spectrum of diesel soot

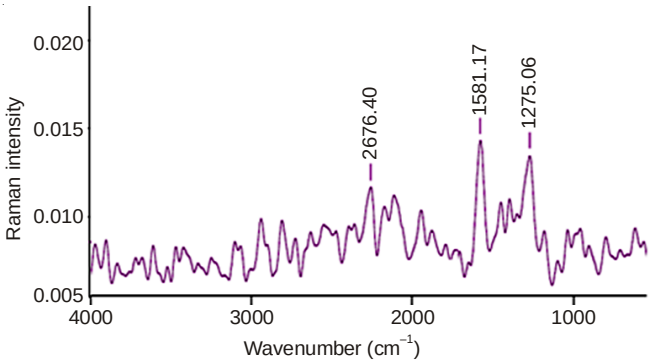

Fig. 6. FT-Raman spectrum of carbon black

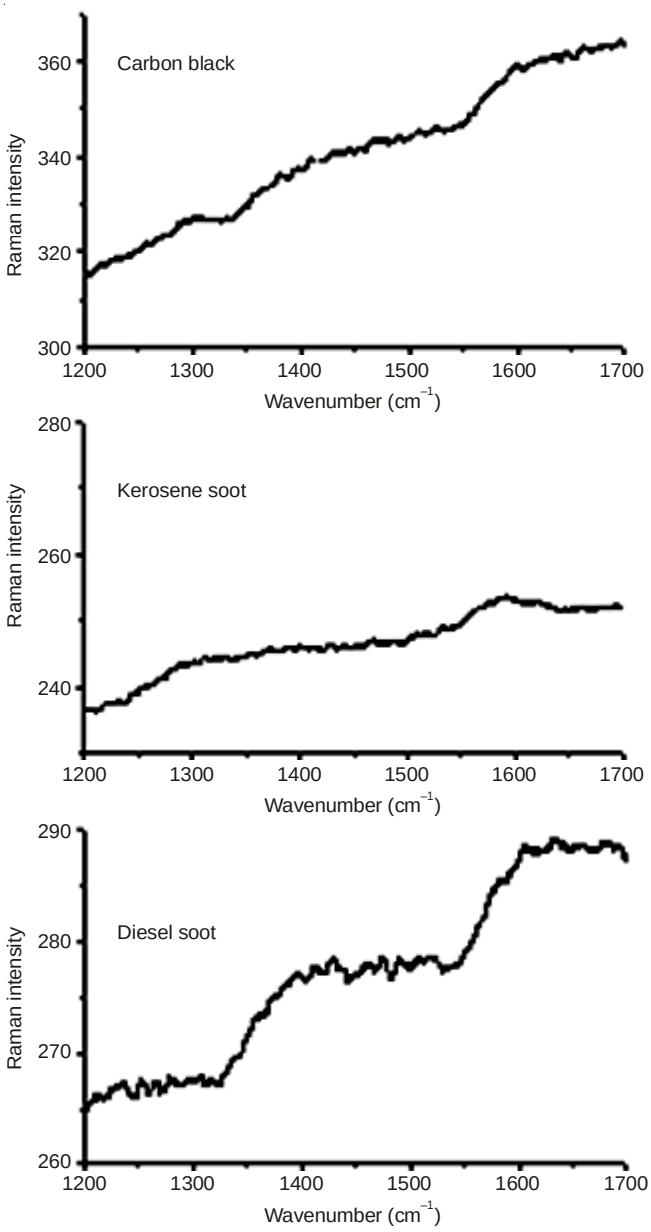

Fig. 7. Raman spectra of samples (wavelength 633 nm)

Raman spectra of samples recorded using 633 nm as the excitation wavelength are depicted in Fig. 7. Broad absorptions are noticed in the 1600-1200 cm^{-1} region. The band observed at 1594 cm^{-1} in kerosene soot is designated as G band. When subjected to laser excitation of 633 nm, the D band is not well resolved. In diesel soot and carbon black, two broad bands are found at the expected D and G band positions.

As the wavelength of laser excitation changes (from 514 to 1064 nm), an uplift in the G-peak position from 1583 to 1610 cm^{-1} is noticed (Fig. 8). Its dispersion is proportionate to the degree of lattice disorder, which is reported to be least in pure graphite and crystalline graphite [1-5,18-21]. I_D/I_G ratio is found to increase with the wavelength of irradiation and is attributed to the resonance character of scattering cross section of D band.

Ferrari and Robertson [13] in their detailed study, reported that nanocrystalline materials tends to obey Tuinstra-Koenig (T-K) relation [13-16]. The average crystallite size of the

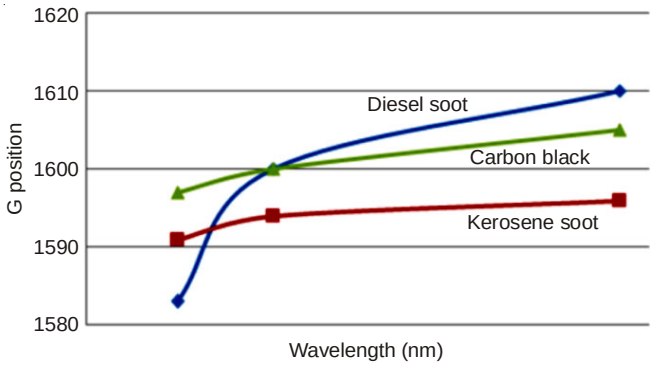

Fig. 8. Dispersion of G peak *versus* excitation wavelength

samples determined using XRD and Raman techniques (Fig. 9) and is presented in Fig. 9, is found to be in good agreement. There exist an inverse correlation between I_D/I_G ratio and L_a (Lateral size). Materials that obey Tuinstra-Koenig relation and are catagorized as nanocrystalline graphite or graphite in the amorphization trajectory [16-22].

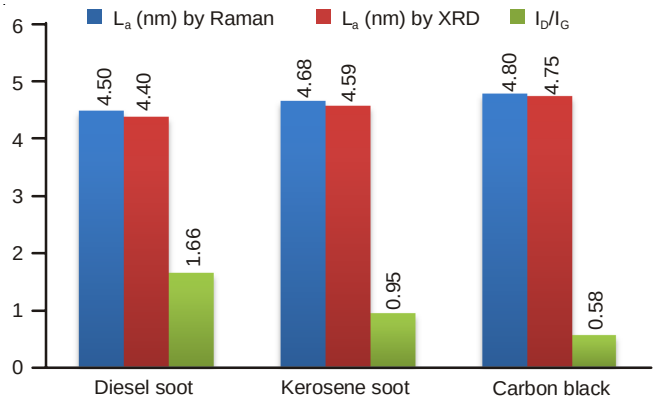

Fig. 9. Comparison of L_a values obtained by Raman and XRD analysis

The integrated intensity ratio of the D and G band (I_D/I_G) is a measure of the quantity of defects in the graphitic materials and is estimated to be 0.95, 1.66 and 0.58 for the kerosene soot, diesel soot and carbon black samples, respectively. The intensity of G band is observed to be uniform over the bulk of the material while the defect (D-band) is confined within the crystal imperfection (typically at the edges or boundary of crystallite). Cancado *et al.* [19] and Lucchase *et al.* [20] independently proposed the value of I_D/I_G~0.8 as the distance between defect approaches zero (L_D~0). In the present study it is noticed that this ratio is found to decrease as the lateral size (L_a) increases. This further support the inference that the defect observed in the nanocrystalline carbon is due to the combination of on-site defect and hopping defect.

Conclusion

The applicability of Raman spectroscopy as a characterization tool for the disordered carbonaceous material is discussed. Raman studies manifested the presence of G band corresponding to the first order scattering of E_{2g} mode. The sp^3 domains at about 1355 cm^{-1} (D band) are attributed to edge planes and disordered structures. Spectral analysis by curve fitting justified the evidence of G, D1, D2, D3 and D4 bands in the first order spectral region. The shape of D3 and D4 bands follows Gaussian, whereas G, D1 and D2 bands are Lorentian. It is observed that with increase in excitation wavelength of laser, the degree of dispersion of G peak and I_D/I_G increases. The crystallite size L_a, show an inverse relation with intensity of defect to graphite band (I_D/I_G) and obey Tuinstra-Koenig relation for nano-crystalline substance. It is found that in carbon black, the defect is mainly due to on-site defect while the defect in the nanolayers of kerosene and diesel soot samples is attributed to the combination of on-site and hopping defects. Raman studies suggest that, kerosene soot, diesel soot and carbon black are potential candidates for excellent electrochemical applications such as super capacitors and sensors.

REFERENCES

1. A. Sadezky, H. Muckenhuber, H. Grothe, R. Niessner and U. Pöschl, *Carbon*, **43**, 1731 (2005).
2. M.A. Pimenta, G. Dresselhaus, M.S. Dresselhaus, L.G. Cancado, A. Jorio and R. Saito, *Phys. Chem. Chem. Phys.*, **9**, 1276 (2007).
3. B. Manoj and A.G. Kunjomana, *Russ. J. Appl. Chem.*, **87**, 1726 (2014).
4. A. Kaniyoor and S. Ramaprabhu, *AIP Adv.*, **2**, 032183 (2012).
5. T. Jawhari, A. Roid and J. Casado, *Carbon*, **33**, 1561 (1995).
6. A. Eckmann, A. Felten, A. Mishchenko, L. Britnell, R. Krupke, K.S. Novoselov and C. Casiraghi, *Nano Lett.*, **12**, 3925 (2012).
7. B. Manoj, *Int. J. Miner. Metull. Mater.*, **21**, 940 (2014).
8. A.N. Mohan and B. Manoj, *Int. J. Electrochem. Sci.*, **7**, 9537 (2012).
9. V. Mennella, G. Monaco, L. Colangeli and E. Bussoletti, *Carbon*, **33**, 115 (1995).
10. R.J. Nemanich and S.A. Solin, *Phys. Rev. B*, **20**, 392 (1979).
11. B. Manoj and A.G. Kunjomana, *Asian J. Mater. Sci.*, **2**, 204 (2010).
12. K. Ramya, J. Jerin and B. Manoj, *Int. J. Elem. Sci.*, **8**, 9421 (2013).
13. A.C. Ferrari and J. Robertson, *Phys. Rev. B*, **64**, 075414 (2001).
14. B. Manoj, *J. Bioremed. Biodeg.*, **6**, (2015); 10.4172/2155-6199.10000306.
15. B. Manoj, *Res. J. Biotechnol.*, **8**, 49 (2013).
16. B. Manoj, *Asian J. Chem.*, **26**, 4353 (2014).
17. B. Manoj and A.G. Kunjomana, *J. Miner. Mater. Charact. Eng.*, **9**, 919 (2010).
18. F. Tuinstra and J.L. Koenig, *Chem. Phys.*, **53**, 1126 (1970).
19. L.G. Cancado, A. Jorio, E.H.M. Ferreira, F. Stavale, C.A. Achete, R.B. Capaz, M.V.O. Moutinho, A. Lombardo, T.S. Kulmala and A.C. Ferrari, *Nano Lett.*, **11**, 3190 (2011).
20. M.M. Lucchese, F. Stavale, E.H.M. Ferreira, C. Vilani, M.V.O. Moutinho, R.B. Capaz, C.A. Achete and A. Jorio, *Carbon*, **48**, 1592 (2010).
21. B. Manoj, *Russian J. Phys. Chem. A*, **89**, 2438 (2015).
22. M. Balachandran, *Am. J. Anal. Chem.*, **5**, 367 (2014).